Published in final edited form as:
Invest Ophthalmol Vis Sci. 2003 October ; 44(10): 4489–4496.

Selective Uptake of Indocyanine Green by Reticulocytes in Circulation

Xunbin Wei[1,2], **Judith M. Runnels**[1,2], and **Charles P. Lin**[1]

[1]Wellman Laboratories of Photomedicine, Massachusetts General Hospital, Harvard Medical School, Boston, Massachusetts

Abstract

Purpose—Hyperfluorescent cells labeled with indocyanine green (ICG) have been observed in retinal and choroidal circulation using scanning laser ophthalmoscopy. It has been suggested that ICG labels leukocytes and that ICG can be used to track leukocyte movement in vivo. The purpose of this study is to identify the cell population that takes up ICG and to study their trafficking pattern in vivo by confocal fluorescence microscopy.

Methods—ICG was injected into the mouse tail vein, and images were taken by in vivo confocal microscopy. The trafficking pattern of ICG-labeled cells was compared with that of rhodamine 6G-labeled leukocytes. In vitro labeling of human blood cells with antibodies against cell lineage markers and with DNA stains was further used to identify the ICG-labeled cells. Antibodies against the following cell surface markers were used: CD45 (leukocytes), CD3 (T lymphocytes), CD19 (B lymphocytes), CD16 (Fc receptor), glycophorin A (erythroid lineage cells), and CD71 (transferrin receptor).

Results—The ICG-labeled cells were made up of two blood cell populations with distinct levels of ICG uptake. The strongly ICG-labeled cells did not roll on dermal vascular endothelium in vivo, in contrast to rhodamine 6G–labeled leukocytes. They were identified as reticulocytes because antibody staining showed that they were CD 45^{-}, glycophorin A^{+} and CD 71^{+}. The weakly ICG-labeled cells were identified as neutrophils because they were $CD45^{+}$, $CD16^{+}$, $CD3^{-}$, and $CD19^{-}$.

Conclusions—ICG strongly labels reticulocytes and weakly labels neutrophils. To the authors' knowledge, this is the first report of selective staining of reticulocytes by ICG.

Indocyanine green (ICG) is a fluorescent dye commonly used in ophthalmology to image retinal and choroidal vasculature. It is also used clinically to measure cardiac output, liver function, and peripheral circulation. Its absorption and emission in the near infrared region allow deep tissue penetration, making ICG angiography particularly useful for imaging choroidal circulation and neovascularization in ophthalmology.[1,2] ICG has provided beneficial information toward identification and treatment regimens in various conditions that manifest retinal or choroidal neovascularization, hemorrhage, or vascular leakage. It has been particularly useful in the management of age-related macular degeneration and idiopathic polypoidal choroidal vasculopathy.[3]

ICG binds to blood plasma proteins immediately after injection and is cleared from the circulation in approximately 20 minutes.[4,5] Recently, Matsuda et al.[6] reported observation of

Corresponding author: Xunbin Wei, BHX 630, Wellman Laboratories of Photomedicine, Massachusetts General Hospital, 50 Blossom Street, Boston, MA 02114; xunbin@helix.mgh.harvard.edu.

[2]Contributed equally to the work and therefore should be considered equivalent senior authors.

Disclosure: **X. Wei**, None; **J.M. Runnels**, None; **C.P. Lin**, None

ICG-labeled cells in retinal and choroidal vessels after dye clearance from the plasma. Based on their size and number, the ICG-labeled cells were thought to be circulating leukocytes. Given the involvement of leukocytes in retinal diseases such as diabetic retinopathy[7] and retinal ischemia,[8] it is important to determine whether leukocyte trafficking can indeed be monitored in vivo by a nontoxic dye such as ICG.

Current fluorescent markers for leukocytes, such as acridine orange (AO) and rhodamine-6G (R6G),[9,10] have significant side effects that affect their use in tracking circulating leukocytes. Both AO and R6G have been demonstrated to be mutagenic or carcinogenic,[11–14] and both may have phototoxic effects.[15–18] Consequently, neither is approved for clinical use. Therefore, it is important to investigate further the use of the nontoxic, clinically approved ICG, as an in vivo circulatory cell stain.

Because image resolution is limited by the optics of the eye, the ICG-labeled cells in the report of Matsuda et al.[6] (imaged with a scanning laser ophthalmoscope) appear as hyperfluorescent dots that are not well resolved. In contrast, in vivo confocal microscopy allows cellular imaging at much higher resolution in the skin (~1-μm transverse and 3–5-μm axial resolution).[19] Here, we used a real-time fluorescence confocal microscope to image cellular uptake of the ICG dye in the dermal microcirculation. In vivo double-labeling experiments using ICG and R6G reveal that two mutually exclusive cell populations take up these dyes. Furthermore, leukocytes labeled with R6G spontaneously roll on dermal vascular endothelium in vivo, whereas ICG-labeled cells do not interact with the dermal endothelium.

To identify the ICG-stained cell population, we used a panel of antibodies against the following cell surface markers: CD45, CD71, CD16, and glycophorin A. CD45 is the leukocyte common antigen that is expressed on all hematopoietic cells not of erythroid lineage. It therefore is present on all leukocytes. Conversely, glycophorin A is expressed exclusively on cells of the erythroid lineage, regardless of developmental stage, whereas CD71 (transferrin receptor) functions in the uptake of iron in immature cells of the erythroid lineage.[20–22] Mature erythrocytes are positive for glycophorin A (glycophorin A^+), but negative for CD45 and CD71 ($CD45^-$ and $CD71^-$, respectively). Reticulocytes (immature erythrocytes in the circulation), are $CD45^-$, glycophorin A^+, and $CD71^+$. We identified the ICG-labeled cells as reticulocytes based on $CD45^-$, glycophorin A^+, and $CD71^+$ immunostaining. In addition, there is a second cell population with distinctly weaker ICG staining that is $CD45^+$ and $CD16^+$. CD16 is a component of the low-affinity Fc receptor that functions in phagocytosis. Fc is the constant region common to all antibodies of a specific class. It was named “crystallizable fragment” because of the discovery of that property in IgG molecules. Unlike the variable antibody regions that recognize and bind to specific antigens, the Fc or constant region is recognized and binds to receptors on phagocytic cells of the immune system such as monocytes, macrophages, and granulocytes. Fc binding to phagocytic cells is critical to the destruction of foreign substance coated by antibodies. We identified these cells as neutrophils based on their $CD45^+$ and $CD16^+$ phenotypes. These weakly labeled cells most likely would not be detected in vivo. To our knowledge, this is the first report of selective and strong reticulocyte staining by ICG.

Materials and Methods

Animal Preparation and In Vivo Fluorescence Confocal Microscopy

Animal experiments were performed in accordance with the Massachusetts General Hospital Subcommittee on Research Animal Care recommendations for the care and use of live animals. All experiments were also performed in accordance with the ARVO Statement for the Use of Animals in Ophthalmic and Vision Research. Young adult female BALB/c mice (5–12 weeks of age) were anesthetized by hind leg intramuscular injection using 80/12 mg/kg body weight ketamine/xylazine. Two or five mg/kg ICG (Akorn, Inc., Buffalo Grove, IL) was injected in

200 to 300 μL sterile H_2O into the tail vein with a 30-gauge needle. The mice were placed on a heated stage (37°C) and imaged for up to an hour after dye injection. For double labeling with R6G and ICG, mice were injected with 6 mg/kg R6G in 100 μL saline, immediately followed by injection of 5 mg/kg ICG in 100 μL water.

Imaging System

A real-time laser scanning confocal and two-photon fluorescence microscope was constructed using a spinning polygon for the fast-scanning axis and a galvanometer-mounted mirror for the slow axis.[19] A mode-locked titanium:sapphire laser (Coherent Mira, Santa Clara, CA; ~ 100 mW at 780 nm) was used for two-photon excitation of the R6G, and the same laser with attenuated output (1–10 mW) was used for one-photon excitation of the ICG. The laser beam was focused to a diffraction-limited spot in tissue (spot size, ~1 μm)[19] using a 30×, 0.9 numerical aperture [NA] water-immersion objective lens (LOMO Optics Inc., Germantown, MD). The field of view was approximately 400 × 300 μm. The fluorescence photons were collected by the same objective lens and spectrally separated by a dichroic filter. The R6G (two-photon-excited) fluorescence was collected by a band-pass filter (535 ± 35 nm) and detected with a photomultiplier tube (Model HC-124-2; Hamamatsu, Hamamatsu City, Japan) without descanning. The ICG (one-photon excited) fluorescence was descanned and separated from the excitation by a band-pass filter (830 ± 20 nm), and detected by an avalanche photodiode (model C5460; Hamamatsu). “Descanning” means directing the remitted (fluorescence) light that originates from a raster-scanned target back through the scanning optics, so that the return beam is stationary again and can be focused through the confocal pinhole. Descanning is not needed for two-photon fluorescence, because the two-photon excitation is restricted to the focal plane of the microscope objective lens. Consequently, there is no out-of-focus fluorescence, and optical sectioning is achieved without the need to reject the out-of-focus light through the confocal pinhole. The photomultiplier tube for the two-photon channel is placed in what is commonly referred to as the “external detector” position. The photomultiplier (two photon channel) and the avalanche photodiode (one photon channel) are both single point detectors with output that contains time-varying signals encoding the two-dimensional image information. Both scanning and image acquisition were computer controlled to produce variable frame rates from 15 to 30 Hz. Signal output was digitized (NI-1408 board, 640 × 480 pixels; National Instruments, Austin, TX) and recorded on digital video tapes (ZR-10; Canon, Tokyo, Japan).

Immunofluorescence Staining

Human peripheral blood was obtained after informed consent was received from five healthy volunteers at the Massachusetts General Hospital. The research involving human subjects adhered to the tenets of the Declaration of Helsinki. Ten to 20 mL of human blood was isolated into K_3EDTA tubes (Vacutainer; BD Biosciences, San Jose, CA). The whole blood was incubated with 12.5 μg/mL ICG for 1 hour at 37°C with occasional mixing in a water-jacketed CO_2 incubator (NAPCO; Precision Scientific, Inc., Chicago, IL). The peripheral white (WBCs) and red (RBCs) blood cells were separated by density centrifugation using a polysucrose solution (Ficoll; Histopaque-1077; Sigma-Aldrich, St. Louis, MO) with a specific gravity of 1.077 g/mL. Briefly, leukocytes were purified by centrifugation on a 5-mL bed of the polysucrose solution for 30 minutes at 55.9 relative centrifugal force (RCF). All cells in the WBC layer or buffy coat were harvested and washed in RPMI-1640 medium containing 5% fetal calf serum (FCS). Most platelets were removed by centrifugation at 14.0 RCF for 10 minutes. After the second centrifugation, the cells were washed twice in PBS, 5% FCS, and 0.1% NaN_3 with centrifugation at 31.4 RCF for 10 minutes. The cells were counted and resuspended in PBS, FCS, and NaN_3 for staining with fluorescent antibodies. The whole peripheral blood or the buffy coat fraction containing the leukocytes was then stained with various monoclonal antibodies (mAbs). A 30-minute incubation at 4°C was used for the

following mAbs: PE-cy5-(phycoerythrin-cyanine fluorochrome 5) conjugated anti-CD16 mAb (clone 3G8) or PE-conjugated anti-glycophorin A mAb (clone GA-R2(HIR2)), respectively. All antibodies were purchased from BD-PharMingen (San Diego, CA) and used according to the manufacturer's instructions. A 30-minute incubation at 4°C was used for the following biotin-conjugated mAbs, followed by a 30-minute incubation of 2 μg/mL cy5-conjugated streptavidin: anti-CD3 (clone HIT3a), anti-CD19 (clone B43), anti-CD45 (clone HI30), or anti-CD71 (clone M-A712). The fluorescence of the ICG and fluorophore-labeled antibodies was examined by confocal microscopy. A 20-minute incubation of 100 nM of a cell-permeating nuclear dye (SYTO-16; Molecular Probes, Eugene, OR) at 4°C was used for DNA and nuclear staining in live cells.

Fluorescence Imaging

Confocal fluorescence imaging of ICG and antibody-labeled cells was performed with the same optical system as described earlier for in vivo imaging, using the Ti:sapphire laser (780 nm) for excitation of ICG. An HeNe laser was used to excite cy5. A mirror mounted on a micropositioning stage was used to direct either the HeNe beam or the Ti: sapphire laser beam into the scanning optics. The cy5 fluorescence was descanned, passed through a 695 ± 27 nm band-pass filter (model XF 3076; Omega Optical, Brattleboro, VT) and a confocal pinhole, and detected by the avalanche photodiode for a one-photon channel, as described previously. All in vitro experiments were performed at 25°C.

Image Analysis and Cell Trafficking Pattern Determination

Fluorescence intensities of the cells were obtained with image-analysis software (NIH Image ver. 1.62a; available by ftp at zippy.nimh.nih.gov/ or at http://rsb.info.nih.gov/nih-image; developed by Wayne Rasband, National Institutes of Health, Bethesda, MD) on a Macintosh G3 computer (Apple, Cupertino, CA). The background was subtracted from the images before analysis. Two-parameter dot plots were made on computer (Kaleidagraph ver. 3.5; Synergy Software, Reading, PA). The images were then processed (NIH Image software or Photoshop ver. 5.0; Adobe Systems Inc., San Jose, CA).

The trafficking pattern of the fluorescent cells was recorded by the real-time in vivo confocal/two-photon microscopy described earlier and analyzed by NIH Image software. The locations of the fluorescent cells were marked on each frame, and the distance between the consecutive fluorescent cells was measured in pixels. The raw data were then processed and plotted on computer (Kaleidagraph, ver. 3.5; Synergy Software). For consistency, only cells trafficking close to the vessel wall were chosen.

Results

Cell Populations Labeled by ICG and R6G In Vivo

To determine whether the ICG hyperfluorescent cells in vivo were leukocytes, we coinjected animals with ICG and the known leukocyte stain R6G.[9,10] Within minutes of dye injection, the ICG-fluorescent dermal vessels in the ear were detected by in vivo confocal microscopy. In the two-photon channel, R6G-stained leukocytes appeared in the circulation (Fig. 1A). R6G-stained leukocytes did not have a detectable level of ICG (Fig. 1B), suggesting that each dye stained a separate population of blood cells.

ICG fluorescence in the plasma decreased exponentially between 10 and 45 minutes after dye injection, and, during this time, ICG hyperfluorescent cells became visible. After 45 minutes, there was little fluorescent signal left in the blood plasma, whereas the hyperfluorescent cells remained visible for approximately 2 hours (Fig. 2A). The movements of ICG hyperfluorescent cells were evaluated by tracking individual cells through a sequence of video frames taken with

in vivo confocal microscopy (Fig. 2B; see supplemental Video A at http://www.iovs.org/cgi/content/full/44/10/4489/DC1) and were found to be significantly different from the typical pattern of R6G-stained leukocytes (see supplemental Video B at http://www.iovs.org/cgi/content/full/44/10/4489/DC1). The ICG-hyperfluorescent cells had a tendency to flow along the vascular wall as leukocytes do, but they did not interact with the endothelium of the blood vessels. In contrast, the R6G-stained leukocytes rolled on postcapillary venules, as previously reported.[10,23,24] Figure 3A shows the tracks (distance versus time) for five typical cells each with either ICG or R6G staining, taken from postcapillary venules of similar diameters. In general, ICG-labeled cells moved along the blood vessels at significantly higher velocities than the R6G-labeled cells did. Moreover, as seen in the expanded plot of Figure 3B, the R6G-labeled cells moved in stepwise fashion typical of rolling interactions with the vascular endothelium. Such interactions were lacking in ICG-labeled cells.

Levels of ICG Uptake In Vitro in Two Blood Cell Populations

The experiments by in vivo confocal two-photon microscopy suggest that ICG labeled-cells are probably not leukocytes. In vitro staining of whole human blood with ICG, however, revealed that there were two populations of cells that took up ICG: one population was brightly labeled with ICG, whereas the second population was at least five times less fluorescent than the first (e.g., Fig. 4D). Therefore, in vitro immunofluorescence was used to identify the ICG-labeled cell populations. The strongly ICG-labeled cells did not possess CD45, the leukocyte common antigen, whereas the weakly ICG-labeled cells were $CD45^+$ (Fig. 4). Furthermore, the strongly ICG-labeled cells did not contain detectable levels of DNA, as shown by live nuclear staining (SYTO-16; Molecular Probes; Fig. 5). On the contrary, the weakly ICG-fluorescent cell contained nuclear DNA.

Identification of Strongly ICG-Fluorescent Blood Cells

The absence of nuclear DNA and CD45 staining in the strongly ICG-labeled cells prompted us to look into the possibility that they were erythroid lineage cells. Indeed, they expressed glycophorin A protein (Fig. 6A), an erythroid cell lineage marker. There are two erythroid lineage cell populations in normal circulating blood: mature RBCs and their precursors, the reticulocytes. The percentage of the ICG-hyperfluorescent cells in the whole peripheral blood correlated well with that known for reticulocytes (~0.5%–1.5%). In addition, the size of the strongly ICG-labeled cells correlated well with that of reticulocytes (~20% larger than RBCs). Further antibody staining showed that the strongly ICG-labeled cells expressed the transferrin receptor CD71 (Fig. 6B). Reticulocytes express CD71, but the CD71 marker is lost when reticulocytes develop into mature RBCs.[21,25] Therefore, the strongly ICG-labeled cells were identified as reticulocytes.

Identification of Weakly ICG-Fluorescent Blood Cells

The presence of CD45 marker on the weakly ICG-labeled cells indicated that they are of the leukocyte lineage. Further immunostaining was used to investigate whether they belong to a specific subpopulation of leukocytes. Cell counting showed that the weakly ICG-labeled cells represented 30% to 70% of the leukocyte fraction. Indeed, the weakly ICG-fluorescent cells expressed the CD16 marker (Fig. 7), an Fc receptor found on neutrophils and natural killer (NK) cells. Because NK cells account for only 1% of total peripheral blood leukocytes, most of the weakly ICG-labeled cells should therefore be neutrophils. Furthermore, the absence of CD3 and CD19 confirmed that the weakly ICG-labeled cells were neither T nor B lymphocytes (Fig. 8).

Discussion

ICG rapidly binds to blood plasma proteins after injection and is cleared from the circulation in approximately 20 minutes. Using in vivo confocal microscopy, we observed circulating cells that took up ICG after the dye was cleared from the blood plasma, confirming the observation of Matsuda et al.,[6] who detected hyperfluorescent cells in the retinal and choroidal circulation using a scanning laser ophthalmoscope. The low abundance of these cells suggested that they were not RBCs. However, in vivo double-labeling experiments with ICG and R6G indicated that they were not WBCs (leukocytes) because cells stained with the established leukocyte stain R6G were not stained by ICG (Fig 1). In addition, R6G-labeled leukocytes roll on dermal vascular endothelium through E- and P-selectin–mediated interactions.[23,24,26] In contrast, the ICG-labeled cells did not interact with the vessel wall. In vitro staining for cell lineage markers and nuclear DNA (using either whole blood or the isolated WBC fraction) led us to conclude that there are two ICG-stained populations. We identified the strongly ICG-labeled cells as reticulocytes and the weakly ICG-stained cells as neutrophils. Most likely only the reticulocytes were detected in vivo, given the weak fluorescence level of neutrophils.

The mechanism of selective ICG uptake by the reticulocytes is not clear. The transferrin receptor is a possible candidate, because it is lost when the reticulocytes develop into mature RBCs.[21,25] However, no correlation was found between the level of ICG uptake and the level of transferrin receptor expression in the reticulocytes observed in this study. Furthermore, neither was any correlation found between the levels of ICG uptake and expression of transferrin receptors in leukocytes. Phagocytic activity may contribute to ICG uptake by the neutrophils.

The selective and strong ICG-staining of reticulocytes opens up the possibility that ICG could be used in research and diagnoses of certain hematopoietic disorders. Patients with disorders such as hairy-cell leukemia, hemolytic anemia, folate deficiency, or sickle cell disease often carry much higher concentrations of reticulocytes in the circulation than healthy individuals.[27,28] In sickle cell disease, some of these cells are thought to be stress reticulocytes. They are prematurely released from the bone marrow to compensate for the stress on the erythroid component of the blood.[29,30] Premature release, however, causes reticulocytes, which still express the vascular leukocyte antigen (VLA)-4 and CD36 (glycoprotein IV) antigens, to circulate,[27] enabling a normally refractive population to attach to vascular cell adhesion molecule (VCAM)-1 on the endothelium,[31,32] as well as the fibronectin,[33] collagen, and thrombospondin components of basement membranes. In the eye, both VLA-4^+ reticulocytes and neutrophils have been demonstrated to bind to retinal vessels,[34,35] and choroidal vessels[33] in the presence of TNFα. Patients with sickle cell disease are known to have elevated cytokine levels in the circulation,[36,37] and the endothelial inflammation markers VCAM-1, intercellular adhesion molecule (ICAM)-1, and P-selectin are induced in the retinal vasculature.[35] Therefore, prematurely released reticulocytes are proposed to be involved in sickle red cell–mediated vaso-occlusion and the resultant retinopathy. The ability to monitor reticulocyte trafficking in vivo will provide insights into the mechanisms involved in such abnormalities. ICG may serve as a specific dye for imaging reticulocytes, to better understand their behavior and contribution to eye complications in sickle cell disease.

Although the strong labeling of the reticulocytes by ICG provides a potential tool to monitor erythropoiesis in vivo—for example, after cancer chemotherapy or in the diagnosis of hematologic disease—the prompt depletion of the ICG-labeled reticulocytes from circulation observed in our study (approximately 2 hours) raises concern for the safety of ICG in certain clinical applications, especially in patients with anemia. ICG may accelerate clearance of the reticulocyte population from the circulation, or clearance of the ICG-stained reticulocytes from circulation may represent normal sequestering of these cells by the spleen during the

reticulocyte maturation process.[38] It has been suggested that the increased proportion of adhesive reticulocytes in the circulation of patients with sickle cell disease compared with patients with other hemolytic disorders may be because many patients with sickle cell disease are asplenic.[27] Hypersensitivity and anaphylactic reactions have been responsible for the most adverse reactions to ICG, yet Benya et al.[39] and Carski[40] stated that 7 of 17 reported reactions occurred in patients with uremia who were undergoing hemodialysis. Identification of the ICG-labeled cells makes it possible to determine the fate of the labeled cells and also to improve understanding of the mechanism of those reactions. Though the mechanisms of these reactions are currently not fully understood, caution should be exercised in ICG application in patients with uremia and anemia who are undergoing hemodialysis. In addition, because the degree of ICG labeling of reticulocytes and possibly their precursors in bone marrow is unknown, the impact of ICG uptake on erythropoiesis should be further investigated. It is clear from our results, however, that ICG is not an appropriate dye for the study of the circulatory patterns of leukocytes in vivo, because ICG brightly stains and makes reticulocytes easily detectable, but not leukocytes.

Supplementary Material

Refer to Web version on PubMed Central for supplementary material.

Acknowledgments

The authors thank Ulrich von Andrian for first pointing out the lack of interactions between ICG-labeled cells and the endothelial wall, and Pat P. Ongusaha, Bernhard Ortel, Salvador Gonzalez, Mehran Poureshagh, Alan R. Prossin, Gerard Lutty, Costas M. Pitsillides, Dorothy A. Sipkins, and Gladys D. Ouedraogo for comments and assistance.

Supported in part by National Eye Institute Grants EY12970 and EY14106 and by the Department of Defense Medical Free Electron Laser Program F4 9620-01-1-0014.

References

1. Slakter JS, Yannuzzi LA, Guyer DR, Sorenson JA, Orlock DA. Indocyanine-green angiography. Curr Opin Ophthalmol 1995;6:25–32. [PubMed: 10151085]
2. Destro M, Puliafito CA. Indocyanine green videoangiography of choroidal neovascularization. Ophthalmology 1989;96:846–853. [PubMed: 2472588]
3. Stanga PE, Lim JI, Hamilton P. Indocyanine green angiography in chorioretinal diseases: indications and interpretation: an evidence-based update. Ophthalmology 2003;110:15–21. quiz 22-13. [PubMed: 12511340]
4. Su MY, Lin DY, Sheen IS, Chu CM, Chiu CT, Liaw YF. Indocyanine green clearance test in non-cirrhotic hepatitis patients: a comparison and analysis between conventional blood sampling method and Finger Piece Monitoring method [in Chinese]. Changgeng Yi Xue Za Zhi 1999;22:17–23. [PubMed: 10418205]
5. Ott P, Keiding S, Bass L. Intrinsic hepatic clearance of indocyanine green in the pig: dependence on plasma protein concentration. Eur J Clin Invest 1992;22:347–357. [PubMed: 1592087]
6. Matsuda N, Ogura Y, Nishiwaki H, et al. Visualization of leukocyte dynamics in the choroid with indocyanine green. Invest Ophthalmol Vis Sci 1996;37:2228–2233. [PubMed: 8843909]
7. Schroder S, Palinski W, Schmid-Schonbein GW. Activated monocytes and granulocytes, capillary nonperfusion, and neovascularization in diabetic retinopathy. Am J Pathol 1991;139:81–100. [PubMed: 1713023]
8. Hatchell DL, Wilson CA, Saloupis P. Neutrophils plug capillaries in acute experimental retinal ischemia. Microvasc Res 1994;47:344–354. [PubMed: 8084299]
9. Becker MD, Kruse FE, Joussen AM, et al. In vivo fluorescence microscopy of corneal neovascularization. Graefes Arch Clin Exp Ophthalmol 1998;236:390–398. [PubMed: 9602324]

10. Nolte D, Hecht R, Schmid P, et al. Role of Mac-1 and ICAM-1 in ischemia-reperfusion injury in a microcirculation model of BALB/C mice. Am J Physiol 1994;267:H1320–H1328. [PubMed: 7943377]
11. Khudolei VV, Mizgirev IV, Pliss GB. Mutagenic activity of carcinogens and other chemical agents in Salmonella typhimurium tests [in Russian]. Vopr Onkol 1986;32:73–80. [PubMed: 3515759]
12. Molnar J, Petofi S, Kurihara T, Sakagami H, Motohashi N. Antiplasmid and carcinogenic molecular orbitals of benz[c]acridine and related compounds. Anticancer Res 1993;13:263–266. [PubMed: 8476222]
13. Martin SE, Adams GH, Schillaci M, Milner JA. Antimutagenic effect of selenium on acridine orange and 7,12-dimethylbenz[alpha]anthracene in the Ames Salmonella/microsomal system. Mutat Res 1981;82:41–46. [PubMed: 6790978]
14. Nestmann ER, Douglas GR, Matula TI, Grant CE, Kowbel DJ. Mutagenic activity of rhodamine dyes and their impurities as detected by mutation induction in Salmonella and DNA damage in Chinese hamster ovary cells. Cancer Res 1979;39:4412–4417. [PubMed: 387214]
15. Saetzler RK, Jallo J, Lehr HA, et al. Intravital fluorescence microscopy: impact of light-induced phototoxicity on adhesion of fluorescently labeled leukocytes. J Histochem Cytochem 1997;45:505–513. [PubMed: 9111229]
16. Zdolsek JM. Acridine orange-mediated photodamage to cultured cells. Apmis 1993;101:127–132. [PubMed: 8387800]
17. Zdolsek JM, Olsson GM, Brunk UT. Photooxidative damage to lysosomes of cultured macrophages by acridine orange. Photochem Photobiol 1990;51:67–76. [PubMed: 2304980]
18. Olsson GM, Brunmark A, Brunk UT. Acridine orange-mediated photodamage of microsomal- and lysosomal fractions. Virchows Arch B Cell Pathol Incl Mol Pathol 1989;56:247–257. [PubMed: 2565619]
19. Rajadhyaksha M, Gonzalez S, Zavislan JM, Anderson RR, Webb RH. In vivo confocal scanning laser microscopy of human skin II: advances in instrumentation and comparison with histology. J Invest Dermatol 1999;113:293–303. [PubMed: 10469324]
20. Hodgson LL, Quail EA, Morgan EH. Iron transport mechanisms in reticulocytes and mature erythrocytes. J Cell Physiol 1995;162:181–190. [PubMed: 7822429]
21. Qian ZM, Morgan EH. Changes in the uptake of transferrin-free and transferrin-bound iron during reticulocyte maturation in vivo and in vitro. Biochim Biophys Acta 1992;1135:35–43. [PubMed: 1591271]
22. Egyed A, Fodor I, Lelkes G. Coated pit formation: a membrane function involved in the regulation of cellular iron uptake. Br J Haematol 1986;64:263–269. [PubMed: 2877685]
23. Nolte D, Schmid P, Jager U, et al. Leukocyte rolling in venules of striated muscle and skin is mediated by P-selectin, not by L-selectin. Am J Physiol 1994;267:H1637–H1642. [PubMed: 7524368]
24. oude Egbrink MG, Janssen GH, Ookawa K, et al. Especially polymorphonuclear leukocytes, but also monomorphonuclear leukocytes, roll spontaneously in venules of intact rat skin: involvement of E-selectin. J Invest Dermatol 2002;118:323–326. [PubMed: 11841551]
25. Johnstone RM. The Jeanne Manery-Fisher Memorial Lecture 1991. Maturation of reticulocytes: formation of exosomes as a mechanism for shedding membrane proteins. Biochem Cell Biol 1992;70:179–190. [PubMed: 1515120]
26. Weninger W, Ulfman LH, Cheng G, et al. Specialized contributions by alpha(1,3)-fucosyltransferase-IV and FucT-VII during leukocyte rolling in dermal microvessels. Immunity 2000;12:665–676. [PubMed: 10894166]
27. Joneckis CC, Ackley RL, Orringer EP, Wayner EA, Parise LV. Integrin alpha 4 beta 1 and glycoprotein IV (CD36) are expressed on circulating reticulocytes in sickle cell anemia. Blood 1993;82:3548–3555. [PubMed: 7505118]
28. Swerlick RA, Eckman JR, Kumar A, Jeitler M, Wick TM. Alpha 4 beta 1-integrin expression on sickle reticulocytes: vascular cell adhesion molecule-1-dependent binding to endothelium. Blood 1993;82:1891–1899. [PubMed: 7691241]
29. Chasis JA, Prenant M, Leung A, Mohandas N. Membrane assembly and remodeling during reticulocyte maturation. Blood 1989;74:1112–1120. [PubMed: 2752157]

30. Noble NA, Xu QP, Hoge LL. Reticulocytes II: reexamination of the in vivo survival of stress reticulocytes. Blood 1990;75:1877–1882. [PubMed: 2184904]

31. Setty BN, Stuart MJ. Vascular cell adhesion molecule-1 is involved in mediating hypoxia-induced sickle red blood cell adherence to endothelium: potential role in sickle cell disease. Blood 1996;88:2311–2320. [PubMed: 8822953]

32. Gee BE, Platt OS. Sickle reticulocytes adhere to VCAM-1. Blood 1995;85:268–274. [PubMed: 7528569]

33. Lutty GA, Otsuji T, Taomoto M, et al. Mechanisms for sickle red blood cell retention in choroid. Curr Eye Res 2002;25:163–171. [PubMed: 12607186]

34. Lutty GA, Taomoto M, Cao J, et al. Inhibition of TNF-alpha-induced sickle RBC retention in retina by a VLA-4 antagonist. Invest Ophthalmol Vis Sci 2001;42:1349–1355. [PubMed: 11328750]

35. Kunz Mathews M, McLeod DS, Merges C, Cao J, Lutty GA. Neutrophils and leucocyte adhesion molecules in sickle cell retinopathy. Br J Ophthalmol 2002;86:684–690. [PubMed: 12034693]

36. Francis RB Jr, Haywood LJ. Elevated immunoreactive tumor necrosis factor and interleukin-1 in sickle cell disease. J Natl Med Assoc 1992;84:611–615. [PubMed: 1629925]

37. Malave I, Perdomo Y, Escalona E, et al. Levels of tumor necrosis factor alpha/cachectin (TNF alpha) in sera from patients with sickle cell disease. Acta Haematol 1993;90:172–176. [PubMed: 8140855]

38. Wyngaarden, JB.; Smith, JH. Cecil Textbook of Medicine. 16th. Philadelphia: WB Saunders Co.; 1982. p. 828-834.

39. Benya R, Quintana J, Brundage B. Adverse reactions to indocyanine green: a case report and a review of the literature. Cathet Cardiovasc Diagn 1989;17:231–233. [PubMed: 2670244]

40. Carski, T. Indocyanine Green: History, Chemistry, Pharmacology, Indications, Adverse Reactions, Investigations and Prognosis: an Investigator's Brochure. Hunt Valley, MD: Becton Dickinson and Co.; 1994.

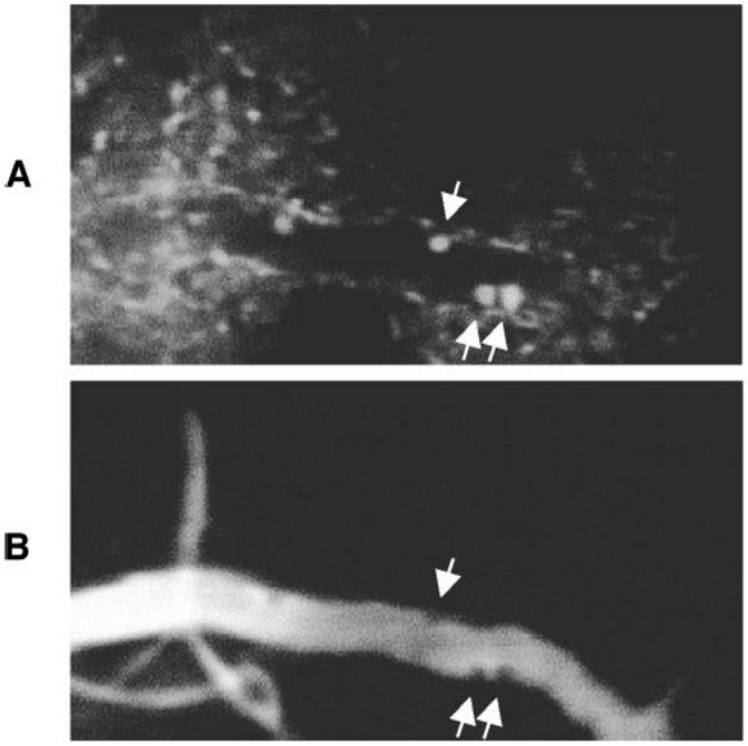

Figure 1.
R6G (**A**) and ICG (**B**) photomicrographs showed that R6G and ICG labeled two different cell populations in vivo, as observed by in vivo confocal two-photon microscopy. R6G and ICG were injected into the same mouse, and the dermal blood vessels of the mouse ear were examined. R6G-stained leukocytes that appeared in the blood vessel (**A**, *arrows*) had no detectable level of ICG (**B**, *arrows*).

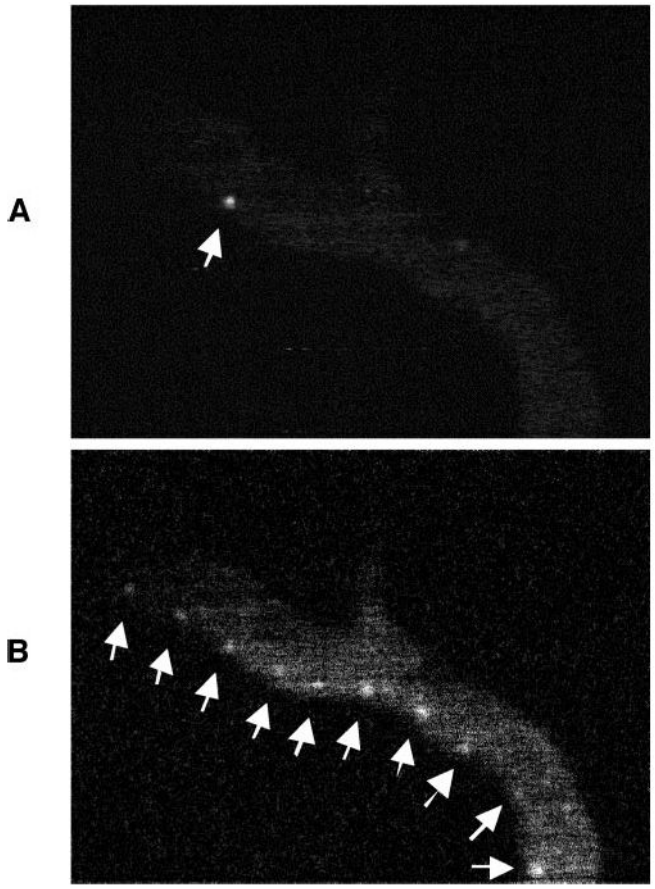

Figure 2.
Time course of the movement of the ICG hyperfluorescent cell (*arrows*) through the dermal vasculature. The movement of an ICG-hyperfluorescent cell (**A**) was evaluated by tracking through a sequence of video frames (**B**) taken with an in vivo confocal microscope.

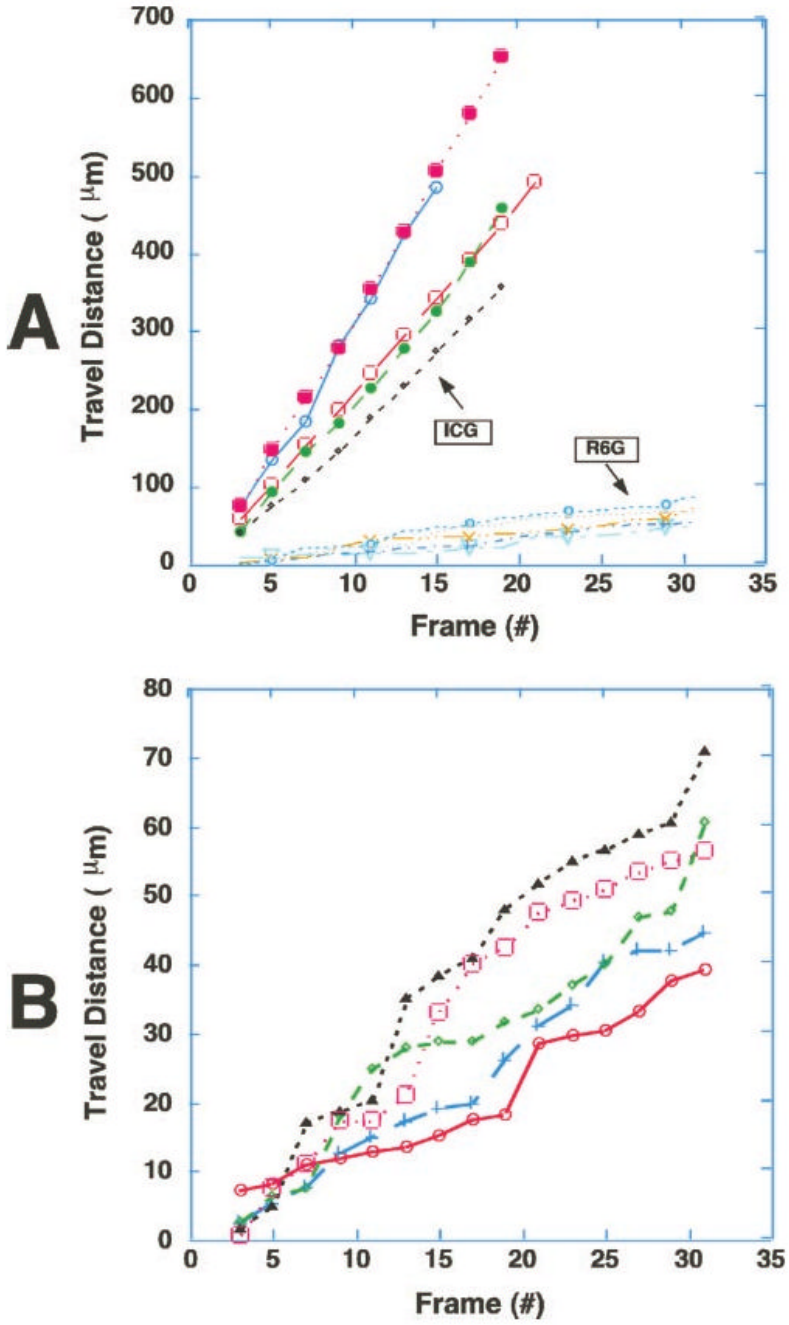

Figure 3.

Trafficking patterns of ICG-hyperfluorescent cells were significantly different from those of R6G-stained leukocytes. The time course of spatial positions of five ICG-hyperfluorescent cells and five R6G-stained leukocytes were plotted from video records (30 frame/sec). Note that the ICG-hyperfluorescent cells were moving much faster than R6G-stained leukocytes (**A**). Furthermore, they were not sticking or rolling on the walls of the blood vessels, in contrast to R6G-stained leukocytes. (**B**) Expanded plot of the R6G-stained cells in (**A**), showing characteristic stepwise movement of leukocytes. Video clips of (**A**) and (**B**) are available at http://www.iovs.org/cgi/content/full/44/10/4489/DC1.

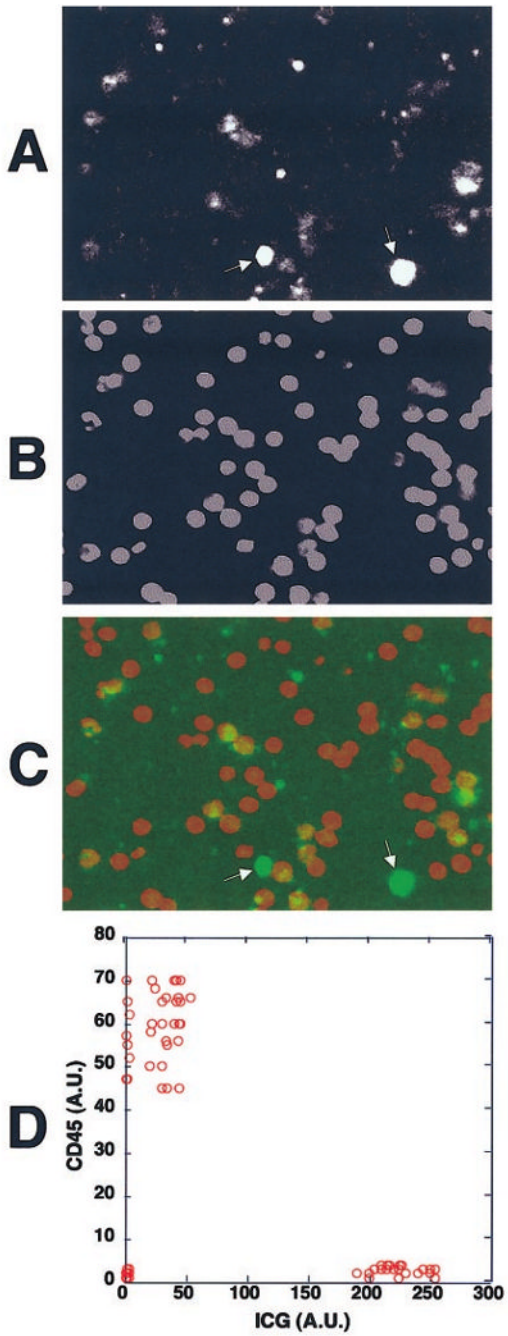

Figure 4.

The strongly ICG-labeled cells were CD45^{-}, and the weakly ICG-fluorescent ones were CD45^{+}. Human whole peripheral blood was incubated with ICG, and the buffy coat fraction containing the leukocytes was isolated. They were then stained with biotinylated anti-CD45 mAb and cy5-tagged streptavidin for examination under the confocal fluorescence microscope. (**A**) The ICG fluorescence of the cells from the WBC fraction. There were two ICG-fluorescent cell populations, one with strong ICG uptake (*arrows*) and one with weak ICG uptake. (**B**) The CD45 staining of the cells shown in (**A**). (**C**) An overlay fluorescence image of ICG (*green*) and CD45 staining (*red*). The strongly ICG-fluorescent cells were CD45^{-} and the weakly fluorescent ones were CD45^{+}. (**D**) The fluorescence intensities of ICG and cy5-tagged anti-

CD45 mAb in each cell were measured and shown in a two-parameter dot plot. Similar results were obtained when whole peripheral blood was incubated with ICG and stained with cy5-tagged anti-CD45 mAb. AU, arbitrary units.

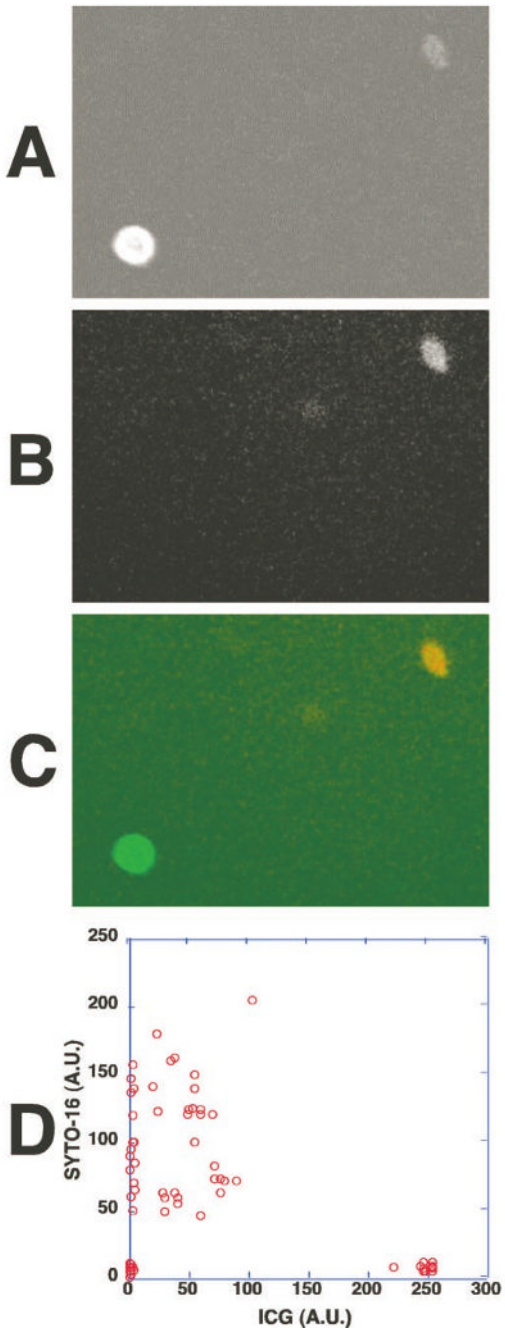

Figure 5.

The strongly ICG-labeled cells did not contain DNA and the weakly ICG-fluorescent cells contained DNA and nuclei. Human whole peripheral blood was incubated with ICG for 1 hour and then stained with a cell-permeating nuclear dye (SYTO-16, Molecular Probes). The fluorescence of ICG and the dye in the cells was examined under the fluorescence microscope. (**A**) ICG fluorescence of the cells in whole peripheral blood. (**B**) The DNA staining of the cells shown in (**A**); 488-nm excitation and 535-nm emission were selected for DNA staining from the nuclear dye's fluorescence. (**C**) An overlay fluorescence image of ICG (*green*) and the nuclear dye (*red*). The strongly ICG-fluorescent cell was SYTO-16 negative, indicating the absence of DNA. A weakly ICG-fluorescent cell contained DNA and a nucleus. (**D**) The

fluorescence intensities of ICG and SYTO-16 fluorescence in each cell were measured and shown in a two-parameter dot plot.

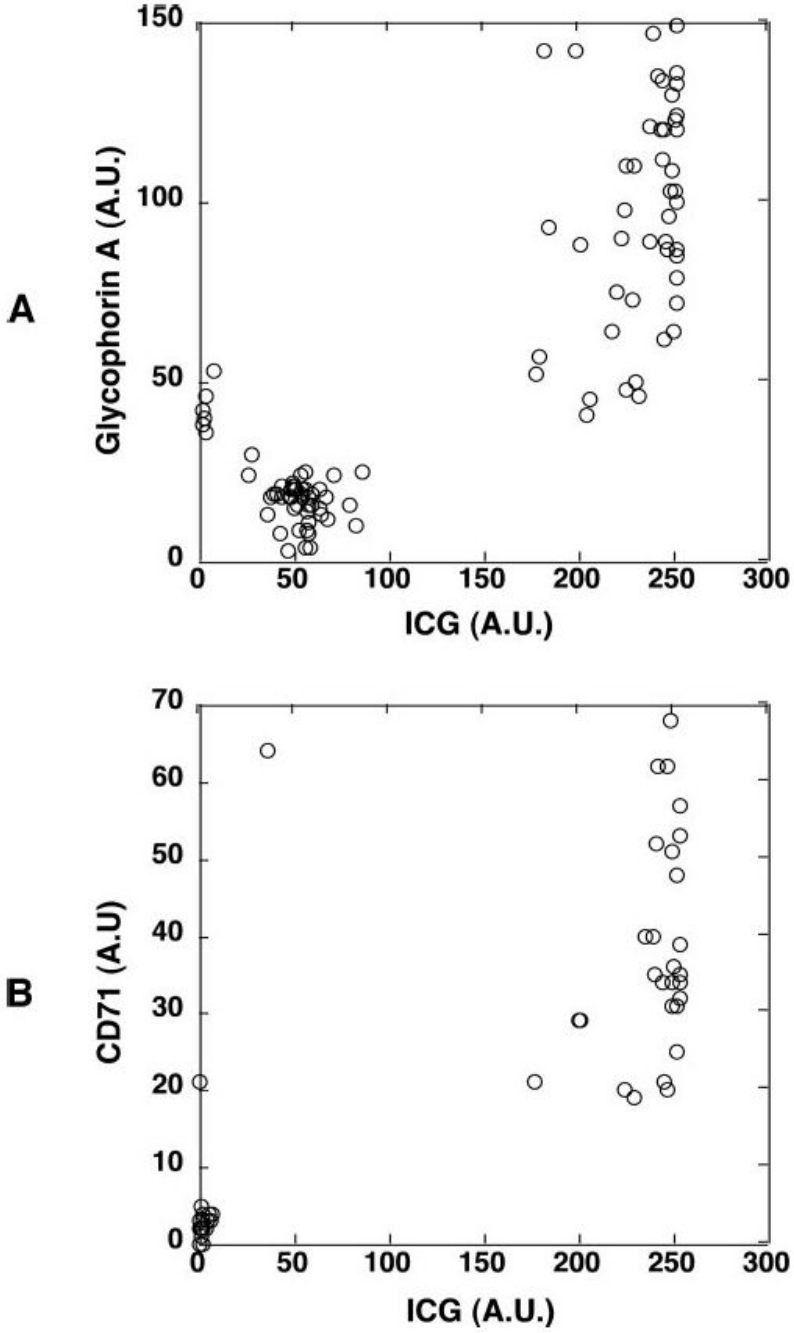

Figure 6.

The strongly ICG-fluorescent cells were reticulocytes. Human whole peripheral blood was incubated with ICG for 1 hour and stained with anti-glycophorin A mAb (PE) or anti-CD71 mAb (cy5). The fluorescence of ICG and fluorophore-labeled mAbs of the cells were examined. (**A**) The fluorescence intensities of ICG- and PE-conjugated anti-glycophorin mAb in each cell were measured and shown in a two-parameter dot plot. The presence of glycophorin A on the strongly ICG-labeled cells indicated their erythroid cell lineage. (**B**) The fluorescence intensities of ICG and cy5-conjugated anti-CD71 mAb in each cell were measured and shown in a two-parameter dot plot. The presence of CD71 marker further indicated that the strongly ICG-labeled cells were reticulocytes. Similar results were obtained when whole peripheral

blood was incubated with ICG, and the leukocytes were isolated, stained with both mAbs, and then examined.

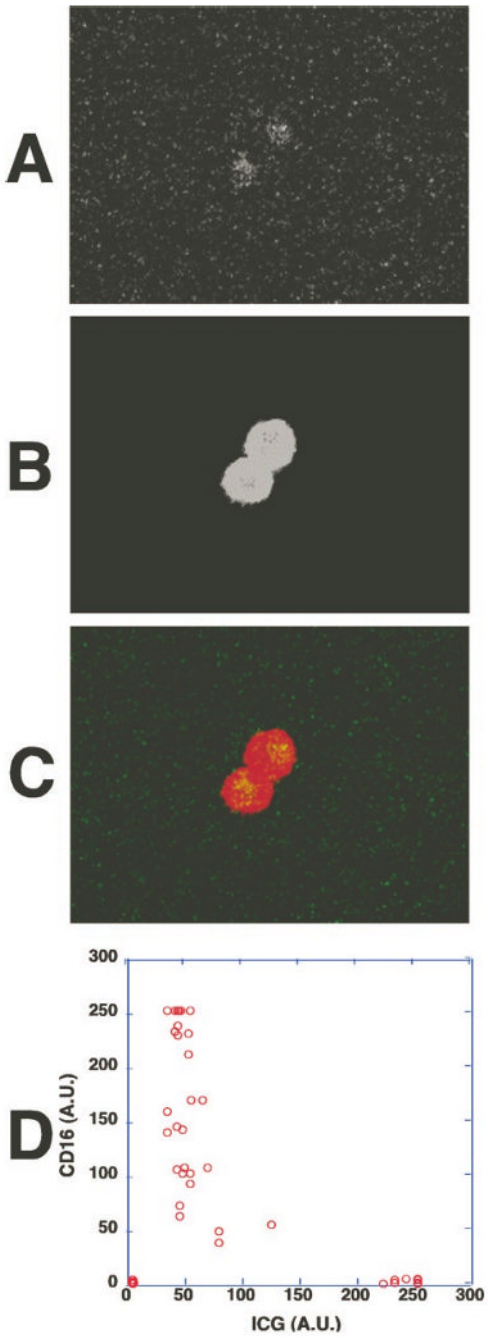

Figure 7.

CD16, a membrane marker for neutrophils and NK cells, was present on the weakly ICG-fluorescent cells. Human whole peripheral blood was incubated with ICG for 1 hour and then stained with cy5-conjugated anti-CD16 mAb. (**A**) ICG fluorescence of the cells from whole peripheral blood examined by fluorescence microscopy. (**B**) Cy5-conjugated anti-CD16 mAb staining of the cells shown in (**A**). (**C**) An overlay fluorescence image of ICG (*green*) and CD16 (*red*). The weakly ICG-fluorescent cells were $CD16^{+}$. (**D**) The fluorescence intensities of ICG and CD16 staining in each cell were measured and shown in a two-parameter dot plot. Similar results were obtained when whole peripheral blood was incubated with ICG and the buffy coat fraction containing leukocytes was isolated, stained with anti-CD16 mAb, and examined.

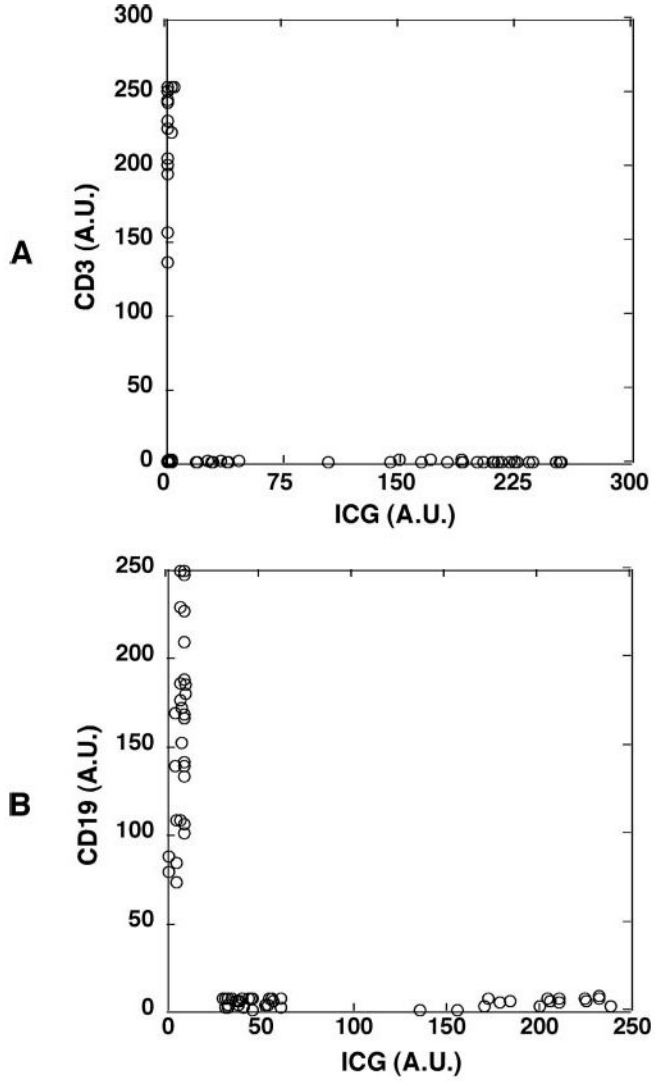

Figure 8.

The weakly ICG-fluorescent cells were confirmed to be neither T lymphocytes nor B lymphocytes. Human whole peripheral blood was incubated with ICG for 1 hour, and the buffy coat fraction containing leukocytes was isolated and stained with mAb against the T lymphocyte marker CD3 or with mAb against the B lymphocyte marker CD19. (**A**) The weakly ICG fluorescent cells were $CD3^{-}$, thus not T lymphocytes. The fluorescence intensities of ICG and cy5-conjugated anti-CD3 mAb in each cell were measured and shown in a two-parameter dot plot. (**B**) The weakly ICG-fluorescent cells were $CD19^{-}$, thus not B lymphocytes. The fluorescence intensities of ICG and cy5-conjugated anti-CD19 mAb in each cell were measured and shown in a two-parameter dot plot. Similar results were obtained when whole peripheral blood was incubated with ICG and stained with both mAbs.